Nearinfrared absorption spectra of 16O3 and 18O3: Adiabatic energy of the 1 A 2 state?

S. M. Anderson, J. Morton, and K. Mauersberger

Near-infrared absorption spectra of $^{16}O_3$ and $^{18}O_3$: Adiabatic energy of the $^1A_2$ state?

S. M. Anderson
Department of Physics, Augsburg College, Minneapolis, Minnesota 55454

J. Morton and K. Mauersberger
School of Physics and Astronomy, University of Minnesota, Minneapolis, Minnesota 55455

New absorption spectra of the $^1A_2 (0,v_2,1) \leftarrow ^1A_1 (0,0,0)$ bands of $^{16}O_3$ and $^{18}O_3$ near 1μ are reported. The behavior of vibronic band isotope shifts for low v_2 suggests that the lowest point on the $^1A_2$ surface lies 9990 ± 70 cm^{-1} above the $^1A_1$ minimum. This result is relatively insensitive to the vibrational assignment. Accounting for zero-point and binding energies of the ground state places the $^1A_2$ minimum very close to the $O + O_2 (v = 0)$ dissociation limit, not low enough to support the zero-point energy of a bound state. Implications regarding recent speculation on the role of this and other electronically excited states in ozone photochemistry are discussed.

I. INTRODUCTION

There are three electronic states of ozone in addition to the $^1A_1$ ground state which correlate with $O(^3P) + O_2 (^3\Sigma^-)$.[1] These are, in order of increasing energy, the $^3B_2$, $^3A_2$ and $^1A_2$. The first of these is believed to have a significant impact on the detailed kinetics of $O + O_2$ recombination,[2] and perhaps on ozone densities at high altitudes.[3] The last may also impact ozone populations in the atmosphere,[4] and has been implicated in observations of transient UV absorption following visible photolysis of ozone.[5,6] To our knowledge, the $^3A_2$ has escaped association with either atmospheric or laboratory phenomena.

These interpretations depend, of course, on whether the state in question is bound. In a recent review of theoretical and experimental evidence, Steinfeld[7] estimated adiabatic excitation energies for the $^3B_2$, $^3A_2$, and $^1A_2$ states, respectively, and concluded that all three might lie below the $O + O_2$ dissociation limit near 1.1 eV. It would be highly desirable to have experimental measurements of these energies.

The work reported here exploits the fact that the $^1A_2 \leftarrow ^1A_1$ transition is spin allowed, and that the C_{2v} symmetry selection rule forbidding the transition is weakened by activity in the asymmetric stretch. Hay and Goddard's assignment[8] of the Wulf bands, first observed 60 years ago,[9] to the vibronically allowed $^1A_2 (v_3 = 1) \leftarrow ^1A_1 (v_3 = 0)$ transition is consistent with the current overall picture of electronically excited states of ozone presented by Steinfeld.[7] These bands have been observed twice since 1930,[10,11] but have never been analyzed. We have therefore undertaken a new study of this system, paying particular attention to the red end of the spectrum and the effect of isotopic substitution on the band positions. Assuming that the electronic assignment is correct, this method allows an unambiguous determination of the adiabatic excitation energy for the $^1A_2$ state.

II. EXPERIMENTAL

Our goal in this work was to determine band positions and isotope shifts for the weak vibronic bands of ozone near 1μ. A low resolution dual-beam spectrometer with a detection limit of 5×10^{-4} fractional absorption at 1 Hz was built for this purpose. Conventional ozone handling techniques allowed us to record multiple spectra for $^{16}O_3$ and $^{18}O_3$ columns of ~ 0.1 atm-m. The apparatus and methods employed to record these spectra are discussed below.

A. Optical system

The dual-beam absorption spectrometer is shown in Fig. 1. White light from a 20 W tungsten lamp was dispersed by a small monochromator and divided into two beams by an achromatic V-mirror beam splitter. An adjustable mask upstream of the splitter was used to balance intensities. The beams were directed through the sample and reference cells, chopped, and finally recombined and imaged through a long-pass filter ($\lambda > 665$ nm) onto a silicon photodiode. The chopper was operated at 257 Hz, and transmitted the reference and sample beams alternately.

The 0.2 m monochromator employed a holographic grating (1200 g/mm, 0.6–1.3 μ) mounted in a custom-built tilter/slit assembly. It was calibrated throughout the wavelength range of interest by recording Ar emission line spectra.[12] For this work, the resolution for isolated lines was 3.2 nm FWHM (triangular), adequate for separating the vibronic bands.

Two identical absorption cells were fabricated from aluminum and equipped with plate glass windows sealed with EPDM O-rings. The windows were angled slightly to avoid
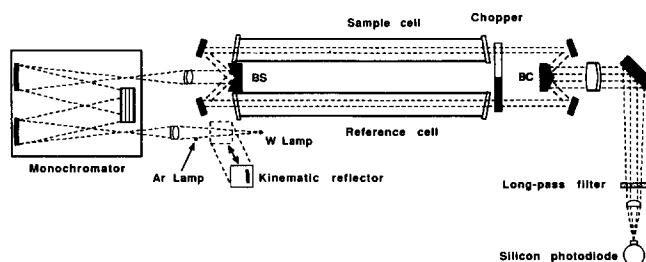

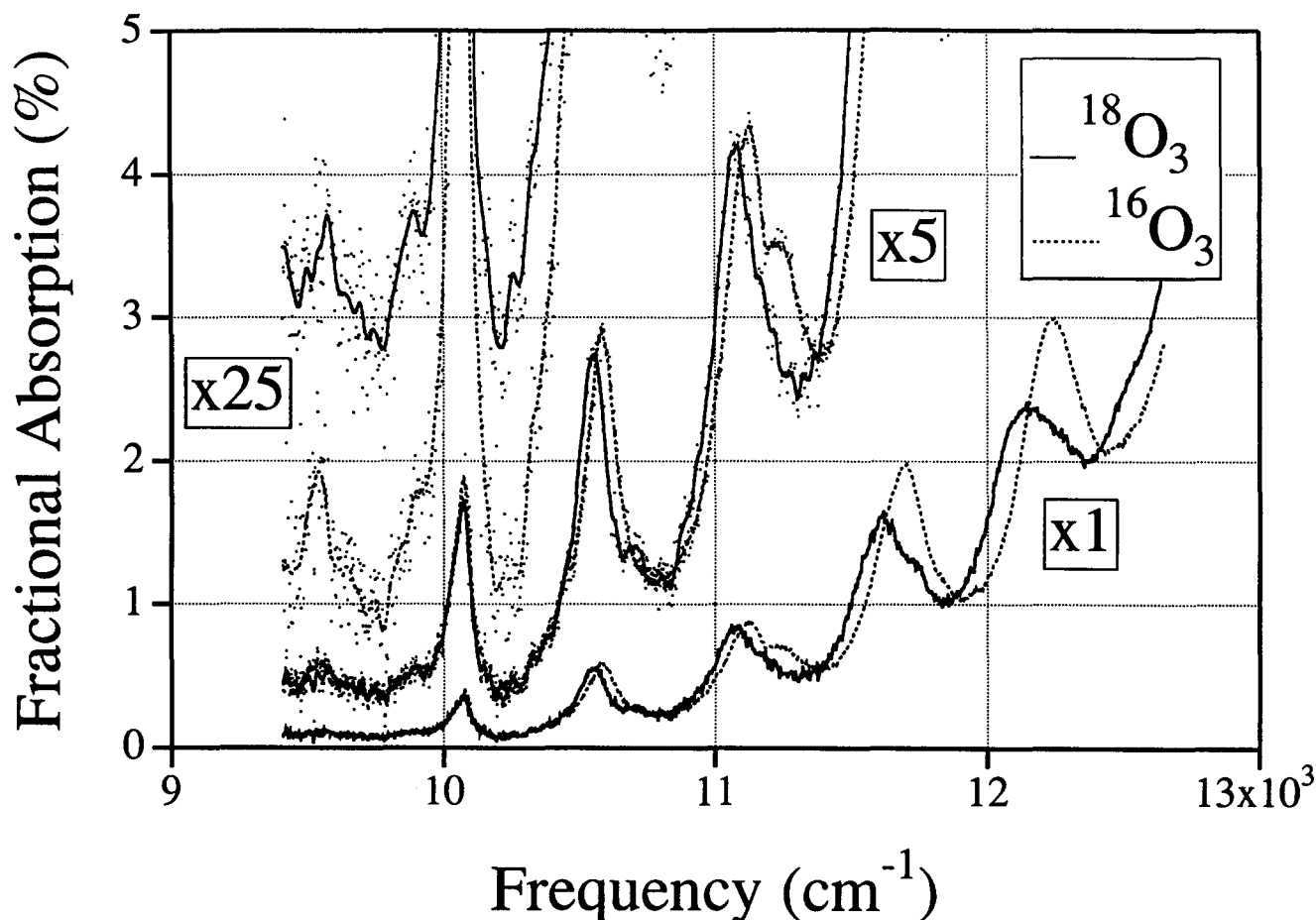FIG. 1. Dual-beam absorption spectro-meter.

FIG. 2. Observed absorption spectra for $^{16}O_3$ (dashed) and $^{18}O_3$ (solid). Monochromator bandwidth (FWHM) was 32 cm^{-1} at 10^4 cm^{-1}, increasing accordingly towards higher energy. Spectra marked $\times 5$ and $\times 25$ have been smoothed (see the text); original data shown as dots. The $\times 25$ traces are offset vertically for clarity.

backreflections. Each cell had a volume of ~ 600 cm^3 and provided an optical path length of 46 cm. The ozone lifetime in the sample cell measured from successive spectra was 2.5 h.

B. Signal processing

Signals from the detector preamp were monitored on an oscilloscope and fed to a pair of synchronously gated integrating amplifiers to obtain simultaneous measurements of the reference beam intensity I_r and the intensity difference between the reference and sample beams, $\Delta I \equiv I_r - I_s$. The gain of the ΔI amplifier was 100-fold greater than that for I_r to enhance sensitivity to small absorptions. The integrator summed 250 chopping cycles per sample, yielding a dwell time of ~ 1 s at each monochromator setting. A personal computer stepped the monochromator between integrations and recorded signals from the amplifier via a 12-bit A/D. These raw scan data were subsequently transferred to another computer for analysis using IGOR software.[13]

Multiple scans recorded with the sample cell empty showed that residual intensity differences along the two beam paths were less than 0.5%, varied slowly over the wavelength range of interest, and were reproducible to better than 0.05%. This background was taken into account in

converting scans recorded with ozone in the sample cell to absorption spectra. Denoting the molecular fractional absorption by $\epsilon \equiv 1 - e^{-\sigma n l}$, the observed background and ozone absorptions are $F = (I_r - I_s)/I_r$ and $f = (I_r - \{1 - \epsilon\}I_s)/I_r$, respectively. From these expressions we find ϵ in terms of F and f:

$$\epsilon = (f - F)/(1 - F). \tag{1}$$

This relation was used to reduce raw absorption signals to molecular absorption spectra.

C. Procedure

$^{16}O_3$ was produced by flowing natural abundance high-purity O_2 (99.995%) through a commercial ozone generator (OREC), and trapped in a Teflon tube immersed in LN$_2$. The trap pressure was kept near 100 Torr to prevent condensation of oxygen; flow rates were adjusted to optimize ozone collection. Ozone was subsequently transferred into the sample cell by warming the trap. The cell was sealed off as soon as the ozone was fully released. The relatively high pressures used here were obtained by sequentially adding several smaller condensed samples to the absorption cell in order to reduce the explosion hazard. To produce $^{18}O_3$ the generator was first evacuated (P < 1 Torr) and filled with
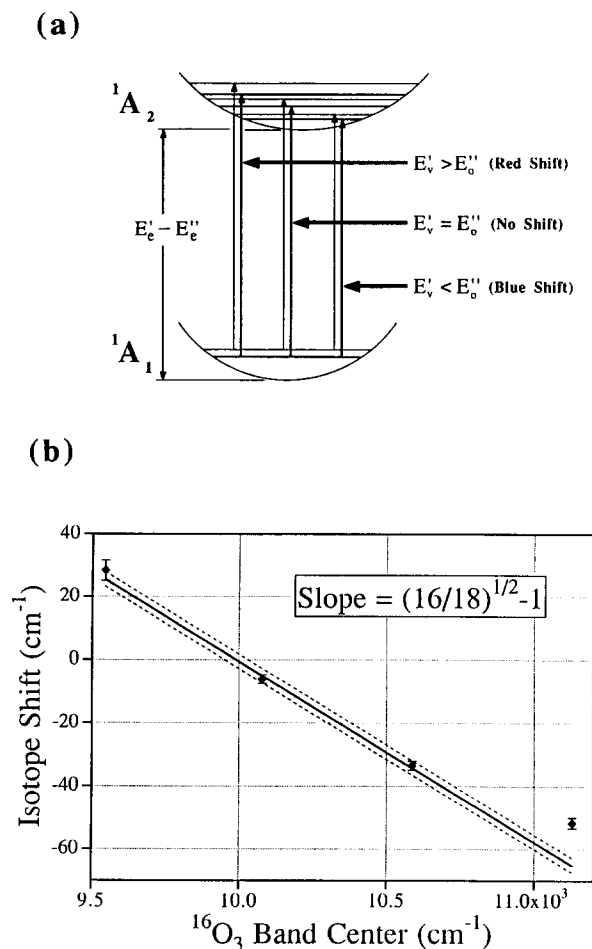
(a)

(b)

FIG. 3. (a) Schematic interpretation of vibronic isotope shifts. (b) Band peak isotope shifts ($\nu_{18} - \nu_{16}$) determined from Fig. 2 vs transition frequency. Lines have slope $\rho - 1$, correspond to pure electronic transition energies of 9990 ± 40 cm^{-1}.

~ 650 Torr of 99 at % $^{18}O_2$ (YEDA). In this case the gas passing through the trap was collected in a tube immersed in LHe, allowing us to recycle nearly all of the isotopic material.

With the desired ozone pressure (≈ 200 Torr) established in the sample cell, several scans were recorded over a preselected wavelength interval. A wavelength step size of 0.25 nm, considerably less than the 3.2 nm resolution of the monochromator, was used throughout. Each scan required about 10 min. Immediately afterwards the cell was pumped out and a matching set of background scans were recorded. This procedure was repeated with the other isotope. Finally, an Ar emission line spectrum was recorded to provide wavelength calibration.[12]

Data for $^{18}O_3$ and $^{16}O_3$ were always taken in matched sets with a common wavelength calibration to eliminate systematic errors in the isotope shifts. Each set was reduced to a pair of absorption spectra by expressing the individual ozone scans as fractional absorption, averaging them together, and combining them with the average background as indicated by Eq. (1). No corrections were applied for ozone decay. For this study two overlapping spectra were combined, accounting for slight differences in ozone density, to yield the working spectrum shown in Fig. 2. In this plot the ×5 and ×25 traces has been smoothed by 5 and 25 passes of a binomial filter, respectively. Due to the relatively high data density this process did not degrade the observed resolution significantly.

The position of each vibronic band was determined by fitting the tip of a Gaussian function to the upper portion of the peak. Typically, data within 20% of the local maximum were included. The precision of this procedure was assessed by repeating the fits for other reasonable sets of data points. The absolute accuracy of the frequency scale is estimated to
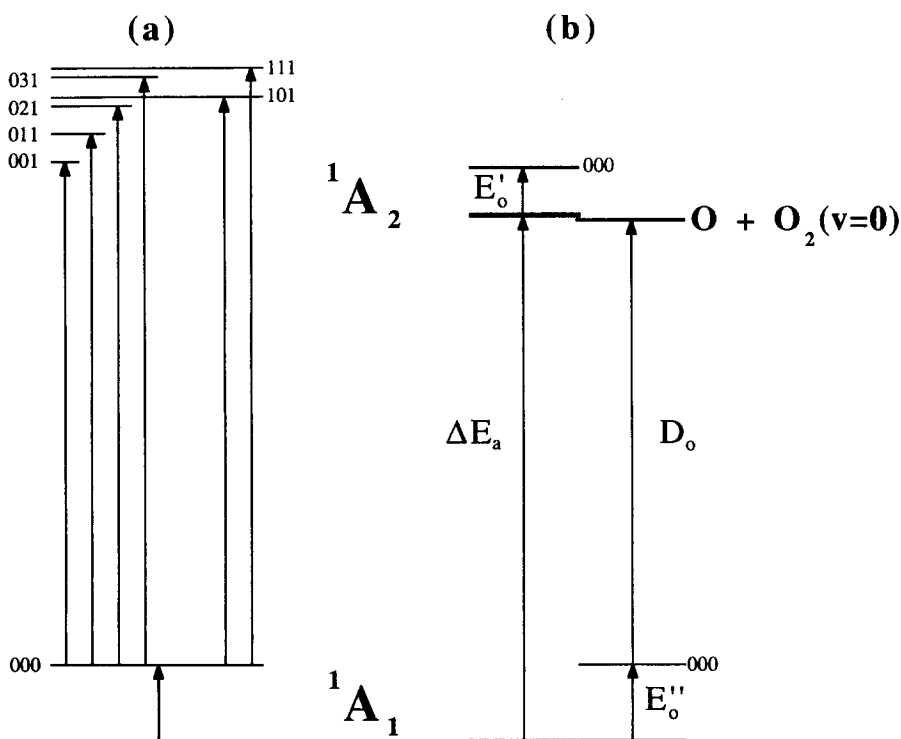
(a)   **(b)**

FIG. 4. Summary of $^1A_2$ energies derived from this work. (a) Spectral assignment. (b) Electronic adiabats with and without zero-point vibrations compared to the O + O₂ dissociation limit.

be < 5 cm^{-1} based on the repeatability of the wavelength calibrations.

III. RESULTS

Three principal results are reported here: (1) a preliminary vibrational assignment, (2) the adiabatic electronic energy of the $^1A_2$ state determined from vibronic isotope shifts, and finally (3) an assessment of the binding energy of $^1A_2$ ozone relative to $O(^3P) + O_2(^3\Sigma^-)$. The methods used to extract this information from the spectra are summarized in Figs. 3 and 4, and discussed in detail below.

A. Spectra

Our interpretation of the spectrum of Fig. 2 follows the work of Pack,[14] who demonstrated that in general a high degree of vibrational structure is expected in the photodissociation of symmetric triatomic molecules. This structure is associated with Franck–Condon factors for the bound degrees of freedom in the upper state, and appears even when that surface is purely repulsive along the dissociation coordinate. In the present case, of course, the v_1 and v_2 modes are bound, while dissociation can only occur along the v_3 coordinate.

The band positions determined from the spectra of Fig. 2 are given in Table I. Those for $^{16}O_3$ generally agree with previously measured values,[9,10] but we observe an additional band at 9544 cm^{-1}, considerably to the red of the origin reported by Wulf.[9] We believe this to be the $(0,0,1) \leftarrow (0,0,0)$ member of the $(0,v_2,1) \leftarrow (0,0,0)$ progression. Our average band separation of 528.2 cm^{-1} compares well with the *ab initio* bending frequency[1] of 537 cm^{-1}, and our $^{18}O_3$ result, 501.5 cm^{-1}, is close to the mass-scaled $^{16}O_3$ band separation of 498 cm^{-1}. Wulf's 566.7 cm^{-1} band spacing appears to have been determined from the higher energy features.

The complex response of these higher bands to ^{18}O substitution suggests that they may arise from a series of progressions such as $(1,v_2,1) \leftarrow (0,0,0)$ and $(2,v_2,1) \leftarrow (0,0,0)$, and/or from participation of a second electronic state (see Sec. IV below). Indeed, the weaker features near 10 750 and 11 250 cm^{-1}, to the blue of the $2v_2 + v_3$ and $3v_2 + v_3$ bands, respectively, could be interpreted as $v_1 + v_3$ and $v_1 + v_2 + v_3$; the similarity of the $(v_1 + v_2 + v_3)/(v_1 + v_3)$ and $(v_2 + v_3)/v_3$ intensity ratios is consistent with this assignment. The resulting symmetric stretching frequency of ~ 1200 cm^{-1} is close to the

ab initio value[1] of 1160 cm^{-1}; we estimate the v_3 frequency following interpretation of the isotopic shifts. This preliminary assignment is summarized in Fig. 4(a); we plan to carry out a more complete analysis including the higher energy features in the near future. For the present purposes, positions for $^{18}O_3$ bands and isotope shifts were determined only for the lower energy transitions whose origins are more certain.

It is worth noting that the widths of the bands increase rapidly with energy. The observed width of the $2v_2 + v_3$ band (105 cm^{-1}), for example, is 25 cm^{-1} larger than that for the nearby $v_2 + v_3$ band (80 cm^{-1}). The monochromator bandwidth increases by only 3 cm^{-1} over this interval (from 33 to 36 cm^{-1}). This may indicate that the lifetime of the upper state decreases rapidly with vibrational energy, consistent with the proximity of these transitions to the dissociation limit, as discussed in Sec. III C below. This may also account for the absence of any obvious progression in higher odd multiples of v_3'.

B. Isotope shifts and electronic energies

To interpret the isotope shifts, we follow convention and write the energy of a given vibronic level as the sum of electronic and vibrational terms[15]

$$T = T_e + \sum_i (v_i + \tfrac{1}{2})\omega_i + \sum_i \sum_k (v_i + \tfrac{1}{2})(v_k + \tfrac{1}{2})x_{ik},$$
(2)

where ω and x are the harmonic and anharmonic constants. The frequencies for transitions originating in the ground vibrational state are

$$\nu = T_e' - T_e'' + \sum_i \left[v_i'\omega_i' + \tfrac{1}{2}(\omega_i' - \omega_i'') \right]$$

$$+ \sum_i \sum_k \left[(v_i' + \tfrac{1}{2})(v_k' + \tfrac{1}{2})x_{ik}' - \tfrac{1}{4}x_{ik}'' \right],$$
(3)

where $'$ and $''$ denote the upper and lower electronic states. The effect of unresolved rotational structure should be small, and is neglected in the present treatment. For full isotopic substitution the vibrational frequencies for the upper and lower states decrease in a simple fashion:[16]

$$\omega_i^* = \rho\omega_i, \quad x_{ik}^* = \rho^2 x_{ik}, \quad \text{with } \rho^2 = m/m^*.$$
(4)

Here m and m^* denote atomic masses for the abundant and rare isotopes, so that $\rho = (16/18)^{1/2} = 0.942\,809$. The electronic energies are unaffected by the change in nuclear masses.

TABLE I. Band positions (peak absorption) for $^{16}O_3$ and $^{18}O_3$. Band identification is number of quanta in upper-state bending mode, v_2''. Uncertainties are 1σ, associated with locating absorption maxima. Estimated absolute accuracy is $\leqslant 5$ cm^{-1}. Wulf values from formula $\nu = 10\,000 + 566.7\,n$ given in Ref. 9; no primary measurements were reported. Lefebvre data from Ref. 10.

Band	ν (Wulf)	ν (Lefebvre)	ν_{16}	$\Delta\nu_{16}$	ν_{18}	$\Delta\nu_{18}$	$\nu_{18} - \nu_{16}$
0	$\cdots$	$\cdots$	$9\,543.8 \pm 2.7$	$\cdots$	$9\,572.1 \pm 1.8$	$\cdots$	$+28.3 \pm 3.2$
1	10 000	10 091	$10\,077.6 \pm 1.0$	533.8 ± 2.9	$10\,071.5 \pm 1.0$	499.4 ± 2.1	-6.1 ± 1.4
2	10 567	10 571	$10\,587.6 \pm 1.1$	510.0 ± 1.5	$10\,554.1 \pm 1.1$	482.6 ± 1.5	-33.5 ± 1.5
3	11 133	11 093	$11\,128.4 \pm 1.2$	540.8 ± 1.6	$11\,076.7 \pm 1.2$	522.6 ± 1.6	-51.7 ± 1.7
4	11 700	11 669	11 701	$\cdots$	$\cdots$	$\cdots$	$\cdots$
5	12 267	12 240	12 246	$\cdots$	$\cdots$	$\cdots$	$\cdots$

For low vibrational levels, we substitute fundamental for harmonic frequencies and drop the anharmonic term, yielding the following expression for the isotope shifts:

$$\Delta \nu \cong (\rho - 1)\left[\left(\frac{1}{2}\sum_i \nu_i' + \sum_i \nu_i'\nu_i'\right) - \frac{1}{2}\sum_i \nu_i''\right] \quad (5)$$

or

$$\Delta \nu \cong (\rho - 1)(E_\nu' - E_0''). \quad (6)$$

To first order, the isotope shifts are controlled by the difference between the vibrational energies in the upper and lower states. In particular, the shift vanishes when these energies are equal, so that the photon energy corresponding to this "shiftless" transition is equal to the adiabatic electronic energy separation. These arguments are summarized in Fig. 3(a), and applied to our data in Fig. 3(b), where we plot the isotope shifts against the observed band peak frequencies. The line of slope $\rho - 1$ fitted to the three lowest energy points passes through zero at a transition energy of 9990 ± 40 cm^{-1}, which we interpret as the adiabatic electronic energy separation between the $^1A_1$ and $^1A_2$ states, ΔE_a. To the uncertainty associated with the fit we add the estimated absolute accuracy of the frequency scale (5 cm^{-1}) and an additional 25 cm^{-1} associated with neglecting possible effects of rotational structure, so that $\Delta E_a = 9990 \pm 70$ cm^{-1}, or 1.24 ± 0.01 eV.

C. Binding energies of $O_3(^1A_2)$

To determine whether a stable bound state forms on the $^1A_2$ surface, we obtain the zero point energy by writing the $(0,0,1) \leftarrow (0,0,0)$ transition energy (9544 cm^{-1}) in terms of the adiabatic separation and the vibrational energies of the ground (1450 cm^{-1}) and excited states:

$$\Delta E_{(001-000)} = \Delta E_a - E_0'' + \frac{1}{2}(\nu_1' + \nu_2' + \nu_3') + \nu_3'. \quad (7)$$

Solving for ν_3' and inserting the other frequencies determined earlier we estimate an insignificantly small asymmetric stretching frequency of 90 ± 80 cm^{-1}. The resulting zero point energy is 910 ± 50 cm^{-1}. The energy of the lowest available vibrational level in the $^1A_2$ state, therefore, lies 10 900 cm^{-1} above the $^1A_1$ minimum.

For comparison, the ozone ground state zero-point vibrational and dissociation energies[17] ($D_0 = 8470 \pm 160$

cm^{-1}) place the $O + O_2(\nu = 0)$ asymptote near 9920 cm^{-1}, very close to the adiabatic energy of the $^1A_2$ state; the lowest quantum level lies 980 cm^{-1} above the dissociation limit. We conclude that the $^1A_2$ surface cannot support a bound state; these results are summarized in Fig. 4(b).

IV. DISCUSSION

We have assumed that Hay and Goddard's electronic assignments,[8] supported by Steinfeld's recent synopsis of all available theoretical and experimental spectroscopic information[7] (summarized in Table II), are correct. The theoretical entries in the table are from Thunemann et al.'s ab initio MRD-CI calculations for vertical excitation energies,[18] and from Hay and Dunning's comprehensive POL-CI-R ab initio calculations[1] of potential energy surfaces, which provide adiabatic as well as vertical excitation energies. Note that Thunemann et al.'s results are consistently lower (by a factor of 0.76 on the average), and in better agreement with experiment. Reasonable adiabatic energies can be estimated by scaling Hay and Dunning's vertical-adiabatic energy differences down to correct for the systematic difference between the two calculations, and then subtracting these from Thunemann et al.'s results. These estimates are given in the sixth column of Table II.[19]

Vaida et al.,[20] however, recently studied the visible absorption spectra of gaseous and condensed-phase ozone, and concluded that the $^1A_2$ transition is better suited to accounting for the Chappuis band system near 17 000 cm^{-1}. This conclusion rests primarily on their measured value of the oscillator strength, $f = 3.2 \times 10^{-5}$. They judged this to be too small by an order of magnitude for the allowed $^1B_1 \leftarrow ^1A_1$ transition usually associated with this band, even though it agrees reasonably well with the ab initio predictions of Hay and Dunning[1] ($f = 4.0 \times 10^{-5}$) and of Thunemann et al.[18] ($f = 1.5 \times 10^{-5}$). Moreover, their reassignment leaves only the $^3B_2$ and $^3A_2$ states for explanation of the Wulf bands, but transitions to these states are spin forbidden from the ground state. It seems to us that association of the Chappuis band with the $^1A_2$ state causes more problems than it solves, and that Steinfeld's assignment is probably closer to the correct one.

Examination of Table II does suggest another candidate, namely the $^3B_1$ state; the estimated adiabatic energy of

TABLE II. Summary of electronic states of ozone based on Steinfeld's review (Ref. 19). Vertical energies from Ref. 18; adiabatic energies estimated from scaled vertical–adiabatic differences fiben in Ref. 1 combined with vertical energies of Ref. 18 (see the text). Experimental energies from Ref. 7.

State	Vertical energy			Adiabatic energy		Assignment
	Ref. 18	Ref. 1	Expt.	Ref. 1	Estimated	
$^3B_2$	1.20	1.60	$\cdots$	0.92	0.68	$\cdots$
$^3A_2$	1.44	2.09	$\cdots$	1.35	0.88	$\cdots$
$^1A_2$	1.72	2.34	1.6	1.66	1.20	Wulf bands
$^3B_1$	1.59	2.01	$\cdots$	1.74	1.39	$\cdots$
$^1B_1$	1.95	2.41	2.1	2.06	1.68	Chappuis bands
$2\,^3B_2$	3.27	4.71	$\cdots$	2.92	1.91	$\cdots$
$2\,^1A_1$	3.60	4.58	$\cdots$	1.20	1.04	(ring state?)
$^1B_2$	4.97	6.12	4.9	5.54	4.53	Hartley bands

1.39 eV is also close to that obtained from our spectra. The $^3B_1 \leftarrow {}^1A_1$ transition is spin forbidden, however, and would probably be much weaker than a vibrationally allowed $^1A_2 \leftarrow {}^1A_1$ transition unless the two upper states interact significantly. *Ab initio* structure calculations[1] suggest that these states are reasonably well separated up to about 0.25 eV above the $^1A_2$ minimum. Mixing would therefore be weak for the lower vibrational levels observed here, but could become significant at higher energies.

Our measurement of the adiabatic energy of the $^1A_2$ state, 9990 ± 70 cm^{-1} (1.24 ± 0.01 eV) is the first experimental determination of this quantity, and the first spectroscopic measurement of any of the low-lying electronically excited states of ozone. Note that although a similar result could have been obtained from the $^{16}O_3$ spectrum alone, it would rely heavily on the correctness of the vibrational assignment. The null isotope shift method employed here depends only on the assumption that the observed bands are associated with low vibrational levels. As previously indicated, our result implies that $^1A_2$ ozone is unstable. Its proximity to the dissociation limit, however, strongly suggests that the lower-lying $^3B_2$ and $^3A_2$ states are bound. This is entirely consistent with the electron energy loss spectrum of Swanson and Celotta,[21] which is principally sensitive to triplet states, and shows a broad peak near a vertical excitation energy of 1.7 eV. These states should be included in theoretical treatments of ozone formation.

McGrath *et al.*[5,6] have reported observations of long-lived transient absorption following flash-pumped dye irradiation of ozone in the Chappuis region, which they attribute to direct photoproduction of $^1A_2$ ozone. Our results are inconsistent with this identification of the absorber. In addition, recent collision-free photodissociation experiments[22] indicate that absorption in the Chappuis region leads to prompt dissociation into translationally hot, ground electronic state products. It is therefore difficult to see how the $^1A_2$ state would be produced by irradiation towards the blue side of the Chappuis band,[5] or how this state could have a lifetime of several milliseconds.[6]

The principal argument presented by McGrath *et al.* to support the photoproduction hypothesis was that no ozone was dissociated during the flash, as determined by the equality of absorption levels prior to and well after lamp firings. No detection limit was specified, however, and it seems plausible that the change in absorption might have been merely small rather than zero. Since the apparent cross sections for the transient were $\sim 10^{-20}$ cm^2, based on the total ozone column, the observed absorption could be explained by the presence of molecules with cross sections 10^3 larger (similar to those in the Hartley band) at a mixing ratio of 10^{-3}. These molecules would presumably have been produced in rapid chemical or energy transfer reactions following the flash, so that the fraction of ozone molecules lost would also be $\sim 10^{-3}$. It seems unlikely to us that the techniques described in McGrath *et al.* would have detected such a small change in absorption.

The transient absorption could therefore arise either from photoproduction of some other state of ozone, or from collisional excitation of ozone by the energy-rich products of the $O + O_3$ reaction. The latter process could occur quite rapidly and therefore escape detection. The chemical lifetime of *thermal* O atoms under their conditions (10–15 Torr of ozone) would be about 0.4 ms, similar to the duration of the flash transient indicated in their paper.[6] It is not clear how long the perturbation of the electronics associated with the flash lamp persists, but closer examination of the rising edge of the absorption's temporal profile would be helpful in detecting precursor chemistry. McGrath *et al.*[5] rejected collisional excitation mechanisms based on the spectral structure of the transient itself, which appears as a well-defined peak 10 nm wide centered at 320 nm. Further study will be needed to find a satisfactory explanation of this phenomenon.

V. CONCLUSIONS

We have used isotope shifts of the lowest vibronic bands of ozone near 1 μ to unambiguously determine the adiabatic energy of the $^1A_2$ state. It lies 9990 ± 70 cm^{-1} (1.24 ± 0.01 eV) above the electronic ground state, very close to the $O + O_2$ dissociation limit. The result is relatively insensitive to the vibrational assignment. Symmetric stretching and bending frequencies measured from the spectra were $\nu_1 \sim 1200$ cm^{-1} and $\nu_2 = 528 \pm 15$ cm^{-1}. Together with the adiabatic energy, these results indicate a small $\nu_3 \sim 90 \pm 80$ cm^{-1}, and a zero-point vibrational energy of 910 ± 50 cm^{-1}. The lowest available quantum state therefore lies 980 cm^{-1} above the dissociation limit, so we conclude that $^1A_2$ ozone is unbound. The $^3B_2$ and $^3A_2$ states, which are believed to lie at significantly lower energies, quite probably *are* bound and should be considered in theoretical modeling of ozone formation.

Further research is needed in several areas. First, although the data of Swanson and Celotta[21] and the present work suggest that the low-lying triplet states are bound, it would be desirable to find spectroscopic evidence for them. This will be difficult since transitions from the ground state are forbidden by spin ($^3B_2$) *and* symmetry ($^3A_2$) selection rules. Second, measurement of the bands studied here with higher sensitivity and resolution, and detection of the hot bands associated with the $^1A_2 \leftarrow {}^1A_1$ transition, would test our preliminary vibrational assignment and provide additional information about the $^1A_2$ surface for comparison with new *ab initio* calculations. Study of the higher energy bands also seems warranted. Finally, closer examination of the transient absorption spectrum observed by McGrath *et al.*[5,6] is needed, since the $^1A_2$ state appears to be dissociative rather than metastable. It would be desirable to determine the true identity of the absorbing species.

[1] P. J. Hay and T. H. Dunning, Jr., J. Chem. Phys. **67**, 2290 (1977).
[2] J. R. Locker, J. A. Joens, and E. J. Bair, J. Photochem. **36**, 235 (1987).
[3] J. A. Joens, J. Geophys. Res. **91**, 14533 (1986).

[4] P. C. Wraight, Planet. Space Sci. **25**, 1177 (1977).

[5] W. D. McGrath, J. M. Maguire, A. Thompson, and J. Trocha-Grimshaw, Chem. Phys. Lett. **102**, 59 (1983).

[6] W. D. McGrath, A. Thompson, and J. Trocha-Grimshaw, Planet. Space Sci. **34**, 1147 (1986).

[7] J. I. Steinfeld, S. M. Adler-Golden, and J. W. Gallagher, J. Phys. Chem. Ref. Data **16**, 911 (1987).

[8] P. J. Hay and W. A. Goddard III, Chem. Phys. Lett. **14**, 46 (1972).

[9] O. R. Wulf, Proc. Natl. Acad. Sci. **16**, 507 (1930).

[10] L. Lefebvre, C. R. Acad. Sci. (Paris) **200**, 1743 (1935).

[11] M. Griggs, J. Chem. Phys. **49**, 857 (1968).

[12] J. Reader and C. H. Corliss, *Wavelengths and Transition Probabilities for Atoms and Atomic Ions I. Wavelengths* (U.S. Natl. Bur. Stand., U.S. Dept. of Commerce, Washington, D.C.), pp. 10–11.

[13] Supplier: Wavemetrics, Lake Oswego, OR.

[14] R. T Pack, J. Chem. Phys. **65**, 4765 (1976).

[15] G. Herzberg, *Molecular Spectra and Molecular Structure, III. Electronic Spectra and Electronic Structure of Polyatomic Molecules* (Van Nostrand Reinhold, New York, 1966), p. 142 ff.

[16] A. Barbe, C. Secroun, and J. P. Jouve, J. Mol. Spectrosc. **49**, 171 (1974).

[17] Natl. Stand. Ref. Data Ser. Natl. Bur. Stand. **37** (1971).

[18] K.-H. Thunemann, S. G. Peyerimhoff, and R. J. Buenker, J. Mol. Spectrosc. **70**, 432 (1978).

[19] There are a some typographical erorrs in Steinfeld's paper. The vertical energies from Ref. 1 for the $^3B_2$, $^3A_2$, and 2 $^3B_2$ states should be 1.60, 2.09, and 4.71 instead of 1.50, 2.12, and 4.17 eV, respectively; that for the $^1A_2$ state from Ref. 18 should be 1.72 instead of 1.59 eV.

[20] V. Vaida, D. J. Donaldson, S. J. Strickler, S. L. Stephens, and J. W. Birks, J. Phys. Chem. **93**, 506 (1989).

[21] N. Swanson and R. J. Celotta, Phys. Rev. Lett. **35**, 783 (1975).

[22] H. B. Levene, J.-C. Nieh, and J. J. Valentini, J. Chem. Phys. **87**, 2583 (1987).